Optics Communications 359 (2016) 195–199

Contents lists available at ScienceDirect

Optics Communications

journal homepage: www.elsevier.com/locate/optcom

Locking of the DFB laser through fiber optic resonator on different coupling regimes

C.A. López-Mercado [a], V.V. Spirin [a,*], J.L. Bueno Escobedo [b], A. Márquez Lucero [b], P. Mégret [c], I.O. Zolotovskii [d], A.A. Fotiadi [c,d,e]

[a] Scientific Research and Advanced Studies Center of Ensenada (CICESE), Carretera Ensenada-Tijuana No. 3918, Zona Playitas, 22860 Ensenada, B.C., Mexico
[b] Centro de Investigacion en Materiales Avanzados, Avenida Miguel de Cervantes 120, Complejo Industrial Chihuahua, C.P. 31109 Chihuahua, Chihuahua, Mexico
[c] University of Mons, Electromagnetism and Telecommunication Department, 31 Boulevard Dolez, B-7000 Mons, Belgium
[d] Ulyanovsk State University, 42 Leo Tolstoy Street, Ulyanovsk 432970, Russia
[e] Ioffe Physico-Technical Institute of the RAS, 26 Polytekhnicheskaya Street, St. Petersburg 194021, Russia

ARTICLE INFO

Article history:
Received 21 July 2015
Received in revised form
1 September 2015
Accepted 22 September 2015
Available online 1 October 2015

Keywords:
Optical resonators
Injection locked oscillators
Optical fibers
Optical feedback

ABSTRACT

We study self-injection locking of DFB laser obtained with a feedback loop that comprises a ring optical fiber cavity. The cavity is tuned to operate in the under-coupled, critically coupled, and over-coupled regimes. The laser operation is found to depend on the cavity coupling regimes. For the locked laser the experimental dependences of the transmitted and reflected from the ring cavity powers are well described by the analytical expressions for the ring cavity only. The best laser stability is observed with critical coupling. In this case the laser power is accumulated inside the cavity providing strong feedback for laser locking and leading to significant narrowing of the laser emitting spectrum. Reduction of the laser linewidth more than 1000 times is demonstrated with the ring cavity operating in under-coupled and critically coupled regimes.

1. Introduction

Further linewidth narrowing of DFB lasers operating at single frequency are of great research interest due to many potential applications [1–4]. The spectral performance of available DFB laser sources could be significantly improved through the use of self-injection locking mechanism [5]. To provide the effect a part of the optical radiation emitted by the laser should be returned back into the laser cavity. This relatively simple method is important for design of cost-effective laser sources demanded by optical fiber communication and sensing [6–8]. The physical events which were observed with optical feedback varied from linewidth narrowing with weak feedback to irregular chaotic oscillations with strong one [6].

Traditional self-injection locking configuration, which is utilized to improve the spectral property of DFB laser, comprises a narrowband pass optical filter inside the weak feedback loop [5]. Current progress in this topic is associated with the use of microcavity techniques [9,10]. By applying optical whispering-gallery-mode resonators, semiconductor lasers with linewidths typically of few hundreds Hz (down to 0.6 Hz, as reported recently [10]) are possible in a rugged, compact, external-cavity configuration. A huge *Q*-factor of cavities used in such systems ($\sim 10^{11}$) is not flexible for tuning. Alternatively, all-fiber cavity approach based on long, but relatively low-*Q*-factor cavities (Fabry–Perot [7] or ring ones [12,13]) is able to provide the similar laser linewidth employing low-cost fiber configuration built from standard telecom components. Such solutions are of particular interest for RF-generation and Brillouin sensing, since the same fiber configuration is able to generate additional waves, providing very high stability in the differences between the generating frequencies [8,12]. The transfer characteristics of the fiber cavities used in different configurations are altered and the minimal laser linewidth is as well varying from tens of kHz [11] down to hundreds of Hz [13]. However, the effect of the fiber cavity characteristics on the efficiency of self-injection locking in DFB laser has not been investigated, yet.

In this work, a low-loss optical fiber ring resonator built from standard telecom components is used as a narrowband filter. Optical waveguide resonators are intensively studied for number of very different applications including signal modulation, optical filtering, dispersion compensation, fiber lasers, wavelength switching and others [14–19]. The optical transfer characteristics of the ring resonator strongly depend on the coupling factor.

* Corresponding author.
E-mail address: vaspir@cicese.mx (V.V. Spirin).

http://dx.doi.org/10.1016/j.optcom.2015.09.076
0030-4018/

Usually three different regimes of the cavity coupling are considered: under-coupling, over-coupling and critical coupling [14–17]. We compare self-injection locking of DFB laser achieved with a feedback loop comprising a ring fiber optic cavity operating at different coupling regimes. Although the laser locking has been achieved in all coupling regimes, we demonstrate that the critical coupling is able to provide the superior laser line narrowing in combination with operation stability.

2. Experimental results and discussion

Experimental configuration of DFB laser employing self-injection locking through a fiber-optic ring resonator (FORR) is shown in Fig. 1. The MITSUBISHI FU-68PDF-V520M27B DFB laser with built-in optical isolator operates at the wavelength ~1534.85 nm. Built-in optical isolator with optical isolation of about 35 dB prevents the influence of unwanted back reflections on laser performance. Without built-in optical isolator, the DFB laser became sensitive to any extremely weak randomly altering reflections from splices, connectors or Rayleigh backscattering. On the other hand a strong reflection or feedback leads to complicate dynamic of the DFB laser output such as periodic or quasi-periodic oscillations, and chaos [6,20]. So, built-in optical isolator completely eliminates uncontrolled weak reflections and Rayleigh scattering and restricts the strong feedback at the same time. This double effect allows studying only the influence of controlled feedback through the FORR on self-injection locking phenomenon at stable regime. The output radiation of the DFB laser is passed through an optical circulator OC, an optical coupler C1, polarization controller PC1 and launched into a fiber-optic ring resonator. The FORR consists of variable rate coupler (VRC), fixed coupler C2 and contains L-m length of standard SMF-28 fiber. The outputs ports A, B and C, with 5 GHz detectors are used for the monitoring of the power of the DFB laser, the reflected and transmitted cavity powers, respectively. Optical isolators (OI) prevent back reflections from the fiber components and detectors that could affect the laser behavior. The optical switcher (OS) is used to switch on/off the optical feedback in the configuration that returns the power transmitted through the FORR back into the DFB laser cavity. The coupler C1 is used to monitor the output power, polarization stability and polarization states of the DFB laser.

When the DFB laser frequency is scanned continuously, the power at the reflected port B exhibits sharp minima each time the laser frequency meets the resonance condition of the ring cavity. Every minimum in the trace of the reflected power is accompanied by a peak in the trace of the power circulating inside the cavity.

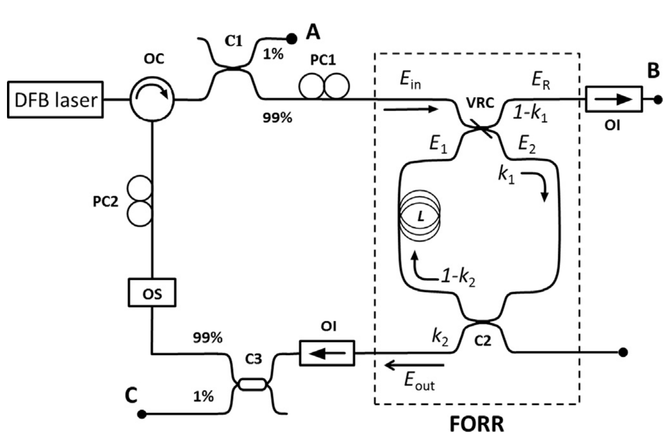

Fig. 1. The experimental configuration; OC – optical circulator, PC – polarization controller, C – coupler, OI – optical isolator, OS – optical switcher, VRC – variable ratio coupler, and FORR – fiber-optic ring resonator.

The circulating power increases until the optical losses inside the ring fiber became equal to the power income from the laser. Generally, the behavior of the FORR is very similar to a linear Fabry–Perot cavity, so ports B and C are equivalent to the reflected and the transmitted ports of the linear cavity, respectively.

In the configuration shown in Fig. 1 the FORR is used as a narrowband optical pass filter included into the feedback loop providing self-injection locking. The total length of the ring cavity is ~4 m that corresponds to a free spectral range (FSR) of ~50 MHz.

Let us assume that the fibers and the couplers inside the FORR are free from polarization coupling and birefringence. In this case the complex field amplitudes E_R and E_2 in steady state are expressed as [14,16]

$$E_R = \sqrt{1-\gamma_1}\left(\sqrt{1-k_1}E_{in} - j\sqrt{k_1}E_1\right) \tag{1}$$

$$E_2 = \sqrt{1-\gamma_1}\left(\sqrt{1-k_1}E_1 - j\sqrt{k_1}E_{in}\right) \tag{2}$$

where κ_1 is the power coupling coefficient and γ_1 is the intensity loss of the variable ratio coupler in a linear scale.

Conservation of energy requires the electric fields E_1 and E_2 to be related as

$$E_1 = \sqrt{\alpha}E_2\exp(-j\omega_P\tau) \tag{3}$$

$$|E_1|^2 = \alpha|E_2|^2 \tag{4}$$

where ω_P is the optical angular frequency, τ is the loop delay time, and α is the power transmission coefficient of the fiber loop.

The power transmission coefficient α includes all losses inside the fiber loop:

$$\alpha = (1-k_2)10^{-(\alpha_0 L+\zeta+\gamma_2)/10} \tag{5}$$

where α_0 is the attenuation coefficient (dB/m) of the fiber, L is the length of the cavity, ζ (dB) is the losses in connectors inside the loop, γ_2 (dB) and k_2 are the intensity loss and power coupling coefficient of coupler C2, respectively.

Let us express the fields inside and outside the FORR as a function of input electric field E_{in}. After some algebraic manipulations with Eqs. (1)–(4) the fields E_1, E_2, E_R can be written as

$$E_1 = \left\{\frac{j\sqrt{\alpha k_1(1-\gamma_1)}}{\sqrt{\alpha(1-k_1)(1-\gamma_1)} - \exp(j\omega_P\tau)}\right\}E_{in} \tag{6}$$

$$E_R = \left\{\frac{\sqrt{\alpha}(1-\gamma_1) - \sqrt{(1-\gamma_1)(1-k_1)}\exp(j\omega_P\tau)}{\sqrt{\alpha(1-\gamma_1)(1-k_1)} - \exp(j\omega_P\tau)}\right\}E_{in} \tag{7}$$

$$E_2 = \left\{\frac{j\sqrt{(1-\gamma_1)k_1}\exp(j\omega_P\tau)}{\sqrt{\alpha(1-\gamma_1)(1-k_1)} - \exp(j\omega_P\tau)}\right\}E_{in}. \tag{8}$$

The output complex field amplitude E_{out} is defined as

$$E_{out} = -j\sqrt{k_2}E_2 \tag{9}$$

In the experiment we measure the intensitiy of the reflected optical radiation at port B and intensity of the transmitted through FORR radiation at port A. In order to validate the experimental data, we find the analytical expressions for the reflected and transmitted intensities. From Eqs. (6) to (9) the expressions for the reflected I_R and transmitted I_{out} intensities normalized on the input intensity I_{in} can be shown as

$$I_R = \left|\frac{E_R}{E_{in}}\right|^2 = (1-\gamma_1)\left\{\frac{\alpha(1-\gamma_1)+(1-k_1)-2\sqrt{\alpha(1-\gamma_1)(1-k_1)}\cos(\omega_P\tau)}{1+\alpha(1-\gamma_1)(1-k_1)-2\sqrt{\alpha(1-\gamma_1)(1-k_1)}\cos(\omega_P\tau)}\right\} \quad (10)$$

$$I_{out} = \left|\frac{E_{out}}{E_{in}}\right|^2 = \frac{k_1k_2(1-\gamma_1)}{1+\alpha(1-\gamma_1)(1-k_1)-2\sqrt{\alpha(1-\gamma_1)(1-k_1)}\cos(\omega_P\tau)} \quad (11)$$

At the resonance $\omega_P\tau = m2\pi$, where m is an integer, the intensity inside the loop and the output intensity I_{out} reaches a maxima:

$$I_{out_{max}} = \frac{k_1k_2(1-\gamma_1)}{(1-\sqrt{\alpha(1-\gamma_1)(1-k_1)})^2}, \quad (12)$$

and the reflected intensity I_R gets the minimum value:

$$I_{R_{min}} = \frac{(\sqrt{\alpha}(1-\gamma_1)-\sqrt{(1-\gamma_1)(1-k_1)})^2}{(1-\sqrt{\alpha(1-\gamma_1)(1-k_1)})^2} \quad (13)$$

The coupling regime is defined by the relation between the coupling coefficient and the losses inside the cavity. When the coupling coefficient $k_1 = 1-\alpha(1-\gamma_1)$, $k_1 < 1-\alpha(1-\gamma_1)$ or $k_1 > 1-\alpha(1-\gamma_1)$, the cavity operates in the critical coupling, under-coupling, and over-coupling regimes, respectively [16].

With the critical coupling condition:

$$k_1 = 1-\alpha(1-\gamma_1) \quad (14)$$

the reflected power $I_{R_{min}}$ becomes equal to zero and all input power is accumulated inside the ring cavity.

Once the DFB laser frequency comes to resonance with the FORR, the DFB laser is locked to the FORR mode. This leads to the suppression of the temporal fluctuations of the powers recorded at ports C and B. The stable power at ports B and C is observed during relatively long time intervals which are interrupted by short-time jumping caused by mode hopping. Fig. 2 shows typical oscilloscope traces for transmitted and reflected powers at the critical coupling regime. Qualitatively the same time-behavior was registered for the under-coupling and over-coupling regimes, but with

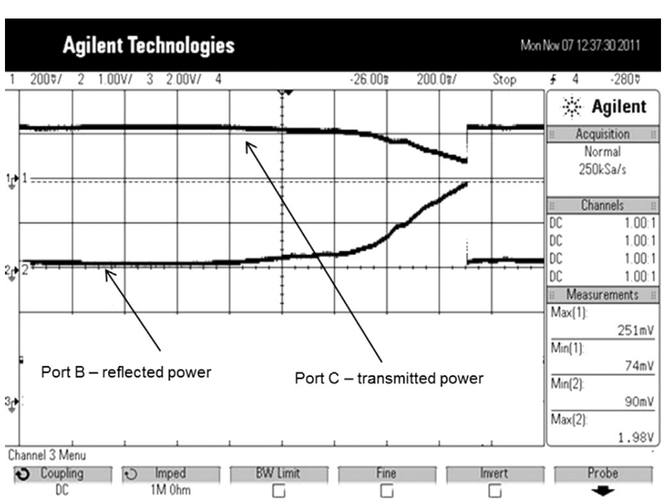

Fig. 2. Typical oscilloscope traces for transmitted and reflected powers at critical coupling regime.

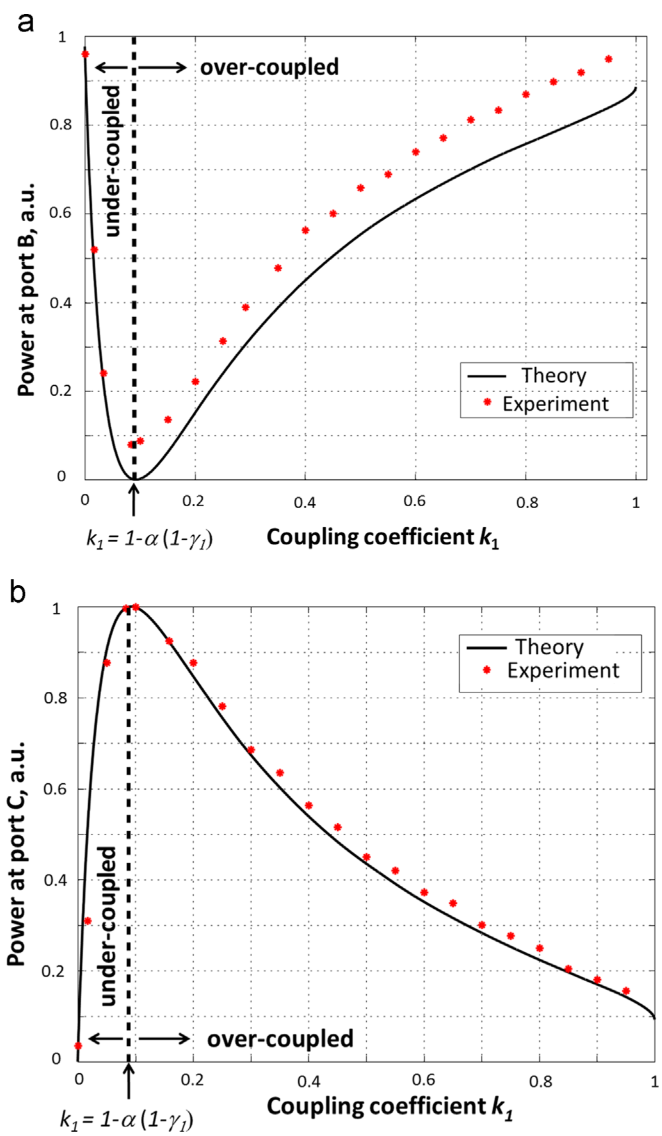

Fig. 3. Reflected (a) and transmitted (b) powers versus coupling coefficient k_1.

shorter stable intervals.

The stable time intervals of 10–30 s with 0.2–0.4 s unstable breaks are typical for the critical coupling regime for unprotected FORR in common lab environment. In the meantime the temporal stability for the under-coupling and over-coupling regimes usually was less and equal to ~5–15 s in our experiment.

In Fig. 3 the dependences of the normalized transmitted and reflected powers on the coupling coefficient k_1 measured at ports B and C are shown in comparison with the data obtained from Eqs. (12) and (13). The following parameters are used for estimations: $k_2 = 0.01$, $\gamma_1 = \gamma_2 = 0.1$ dB, $\zeta = 0.2$ dB and $\alpha_0 = 0.17$ dB/km. The reflected power reaches zero at $k_1 = 0.08$, that corresponds to the critical coupling. In the experiment we tune the variable rate coupler VRC to get the ring cavity to operate at the three different regimes: under-coupling, over-coupling and critical coupling.

Both the experimental and calculated dependences for reflected powers exhibit minimum at $k_1 = 0.08$. Experimentally, however, we never reach zero for the transmitted power in the critical coupling regime, in spite of careful polarization adjustment. We suppose that this effect is due to undesirable polarization coupling and small birefringence of the fiber constituting the FORR that make impossible to get a complete destructive interference by means of the variable rate coupler. As a result all

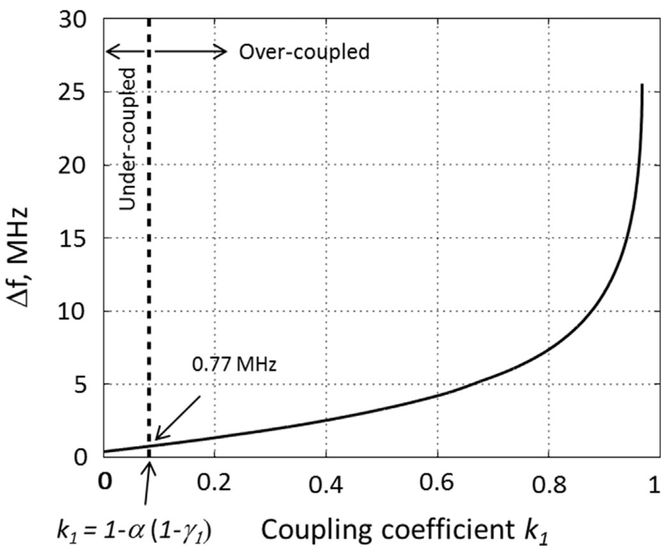

Fig. 4. Linewidth of the resonance mode of FORR versus coupling factor k_1.

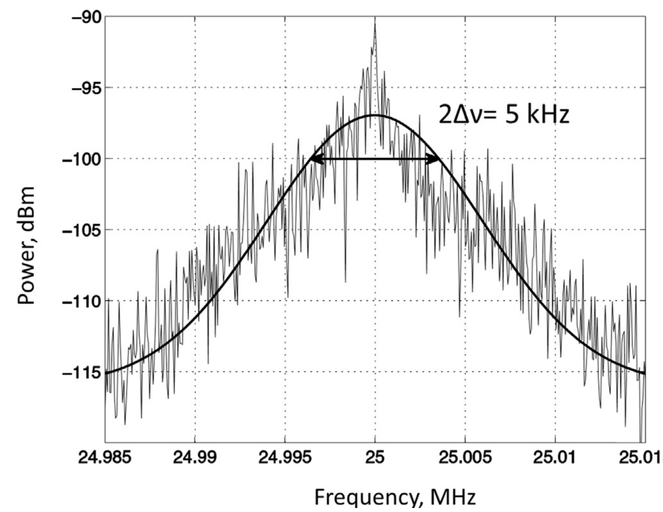

Fig. 5. Delayed self-heterodyne spectra of the locked DFB laser for the critical coupling.

experimental points for over-coupling regime lies above the theoretical curve (see Fig. 3a). Nevertheless, normalized experimental and calculated transmitted powers perfectly coincide (see Fig. 3b).

The finesse of the resonance peak of the FORR is defined as the ratio of the resonance peak spacing to the frequency bandwidth that is

$$\mathcal{F} = \mathrm{FSR}/\Delta f \tag{15}$$

where $\mathrm{FSR}=c/nL=1/\tau \approx 50$ MHz is the free spectral range of the FORR and Δf is the full-width at half-maximum (FWHM) of the loop intensity.

For our direct coupled configuration of the FORR with additional coupler C2 Δf can be found from Eqs. (12) to (14) by the same procedure as in Ref. [16] for the simple cross-coupled optical ring resonator. For our resonator, the FWHM of the cavity mode can be estimated as

$$\Delta f = \frac{1}{2\pi\tau}\cos^{-1}\left(2 - \frac{1 + \alpha(1-\gamma_1)(1-k_1)}{2\sqrt{\alpha(1-\gamma_1)(1-k_1)}}\right) \tag{16}$$

Fig. 4 shows the linewidth dependence of the FORR resonance mode Δf on the coupling coefficient k_1 calculated from Eq. (16). For the critical coupling $k_1=0.08$ $\Delta f=0.77$ MHz and the finesse $\mathcal{F} = 65.8$.

In the experiment we use a delayed self-heterodyne technique to measure the linewidth of radiation emitted by the laser at port A. An all-fiber spliced Mach–Zehnder interferometer with a 15 km delay fiber in one arm and 25 MHz phase modulator supplied by polarization controller in the second arm is used for this purpose. The beat signal from the interferometer is detected by a 1 GHz photodiode and RF spectrum analyzer. With assumption that the line shape is Lorentzian, the delayed self-heterodyne spectrum width is simply twice measured laser linewidth [21]. The linewidth at half-maximum of the free running DFB laser is estimated to be equal to 2.55 MHz.

Self-injection locking results in a drastic reduction of the laser linewidth. Fig. 5 shows the delayed self-heterodyne spectra of the locked laser for the critical coupling $k_1=0.08$. It should be noted that the delay length equal to 15 km is too short to obtain the incoherent mixing which is required in the delayed self-heterodyne technique. For the 2.5 kHz linewidth the length of the delay fiber should exceeds 20 km. However, the error due to shorter delay fiber can leads to visible large-scale oscillation in self-heterodyne spectra and to an increase of the estimated linewidth in comparison with actual one [21]. For that reason, the actual linewidth of the locked laser with critical coupling does not exceed the measured value equal to 2.5 kHz.

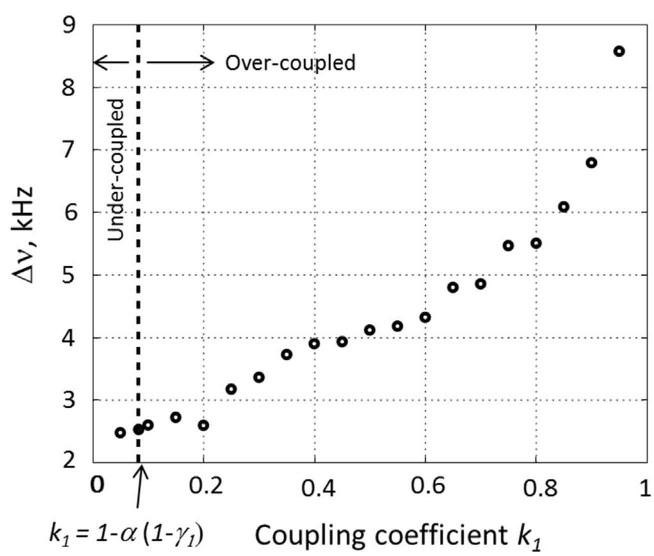

Fig. 6. Linewidth of the locked DFB laser versus coupling factor k_1.

Fig. 6 presents the linewidth of the locked DFB laser versus the coupling factor k_1. The laser linewidth strongly depends on the coupling conditions; it reduces more than 1000 times in under-coupling and critical coupling regimes, but much less in over-coupling regime. Let us emphasis that linewidth of the locked laser is significantly less than the width of the cavity mode (see Fig. 4). So, we cannot conclude that the laser linewidth is completely defined by the pass-band of the filter. However, the behavior of the experimental dependence of the laser linewidth shows that it demonstrates similar tendencies (see Figs. 4 and 6).

The locking phenomenon was experimentally recorded for all coupling regimes but the critical coupling provides more stable locking regime. We believe that the locking stability can be further improved by utilizing fully PM fiber spliced configuration and temperature stabilization of the FORR.

3. Conclusion

We have utilized low-loss fiber optical ring resonator with an ordinary SMF-28 communication fiber and directional couplers as a high finesse filter for the self-injection locking of the DFB laser. By varying the coupling coefficient, we have compared the laser locking with FORR operating in the under-coupled, critically coupled, and over-coupled regimes. For the locked laser, the transmitted and reflected powers from FORR are in good agreement with the theoretical estimations. The critical coupling provides higher feedback powers leading to better locking and also delivers superior narrowing of the laser linewidth. We have demonstrated that locked DFB laser generates single-frequency radiation with linewidth less than 2.5 kHz as the FORR operates in the critically coupled regime. The laser linewidth increases significantly in the over-coupled regime. We believe that these results are important for designing new single frequency lasers employing self-injection locking phenomena, including lasers based on advanced micro-cavity techniques.

Acknowledgments

The work was supported by CONACYT (265517), Mexico, the IAP program VII/35 of the Belgian Science Policy and Ministry of Education and Science of Russian Federation (14.Z50.31.0015, RFMEFI57414X0057).

References

[1] Q. Li, F.P. Yan, W.J. Peng, G.L. Yin, T. Feng, S.Y. Tan, S. Liu, A single frequency, linear cavity Tm-doped fiber laser based on phase-shifted FBG filter, Opt. Laser Technol. 56 (2014) 304–306.

[2] J.Z. Sotor, G. Dudzik, K.M. Abramski, Single frequency, monolithic Nd:YVO_4/YVO_4/KTP diode pumped solid state laser optimization by parasitic oscillations elimination, Opt. Commun. 291 (2013) 279–284.

[3] S.A. Babin, D.V. Churkin, A.E. Ismagulov, S.I. Kablukov, M.A. Nikulin, Single frequency single polarization DFB fiber laser, Laser Phys. Lett. 4 (6) (2007) 428–432.

[4] Y. Ge, S. Guo, Y. Han, J. Wang, Realization of 1.5 W 780 nm single-frequency laser by using cavity-enhanced frequency doubling of an EDFA boosted 1560 nm, Opt. Commun. 334 (2015) 74–78.

[5] B. Dahmani, L. Hollberg, R. Drullinger, Frequency stabilization of semiconductor lasers by resonant optical feedback, Opt. Lett. 12 (11) (1987) 876–878.

[6] J. OthsubO, Semiconductor Laser, Stability, Instability and Chaos, 2nd ed., Springer-Verlag, Berlin, Heidelberg, 2008.

[7] X.H. Li, X.M. Liu, Y.K. Gong, H.B. Sun, L.R. Wang, K.Q. Lu, A novel erbium/ytterbium co-doped distributed feedback fiber laser with single-polarization and unidirectional output, Laser Phys. Lett. 7 (1) (2010) 55–59.

[8] L. Thevenaz, S. Le Floch, D. Alasia, J. Troger, Novel schemes for optical signal generation using laser injection locking with application to Brillouin sensing, Meas. Sci. Technol. 15 (2004) 1519–1524.

[9] W. Liang, V.S. Ilchenko, A.A. Savchenkov, A.B. Matsko, D. Seidel, L. Maleki, Whispering-gallery-mode-resonator-based ultranarrow linewidth external-cavity semiconductor laser, Opt. Lett. 35 (16) (2010) 2822–2824.

[10] W. Liang, V.S. Ilchenko, D. Eliyahu, A.A. Savchenkov, A.B. Matsko, D. Seidel, L. Maleki, Ultralow noise miniature external cavity semiconductor laser, Nat. Commun. 6 (2015) 7371, http://dx.doi.org/10.1038/ncomms8371.

[11] A. Zhang, X. Feng, M. Wan, Z. Li, B. Guan, Tunable single frequency fiber laser based on FP-LD injection locking, Opt. Express 21 (2013) 12874–12880.

[12] V.V. Spirin, M. Castro, C.A. López-Mercado, P. Mégret, A.A. Fotiadi, Optical locking of two semiconductor lasers through high order Brillouin Stokes components in optical fiber, Laser Phys. 22 (4) (2012) 760–764.

[13] V.V. Spirin, C.A. López-Mercado, P. Mégret, A.A. Fotiadi, Single-mode Brillouin fiber laser passively stabilized at resonance frequency with self-injection locked pump laser, Laser Phys. Lett. 9 (2012) 377–380.

[14] L.F. Stokes, M. Chodorow, H.J. Shaw, All-single-mode fiber resonator, Opt. Lett. 7 (6) (1982) 288–290.

[15] M. Sumetsky, Y. Dulashko, A. Hale, Fabrication and study of bent and coiled free silica nanowires: self-coupling microloop optical interferometer, Opt. Express 12 (15) (2004) 3521–3531.

[16] Faramarz E. Seraji, Steady-state performance analysis of fiber-optic ring resonator, Prog. Quantum Electron., 33, (2009) 1–16.

[17] P.P. Yupapin, P. Saeung, C. Li, Characteristics of complementary ring-resonator add/drop filters modeling by using graphical approach, Opt. Commun. 272 (2007) 81–86.

[18] V.V. Spirin, C.A. Lopez-Mercado, D. Kinet, P. Megret, I.O. Zolotovskiy, A. A. Fotiadi, A single-longitudinal-mode Brillouin fiber laser passively stabilized at the pump resonance frequency with a dynamic population inversion grating, Laser Phys. Lett. 10 (2013) 015102.

[19] V.V. Spirin, C.A. Lypez-Mercado, S.I. Kablukov, E.A. Zlobina, I.O. Zolotovskiy, P. Megret, A.A. Fotiadi, Single cut technique for adjustment of doubly resonant Brillouin laser cavities, Optics Lett. 38 (14) (2013) 2528–2530.

[20] L. Cardoza-Avendaño, V. Spirin, R.M. López-Gutiérrez, C.A. López-Mercado, C. Cruz-Hernández, Experimental characterization of DFB and FP chaotic lasers with strong incoherent optical feedback, Opt. Laser Technol. 43 (2011) 949–955.

[21] D.M. Baney, W.V. Sorin, High resolution optical frequency analysis, in: D. Derickson (Ed.), Fiber Optic Test and Measurement, Prentice-Hall PTR, 1998, pp. 169–219.